Optical cavities and waveguides in hyperuniform disordered photonic solids

Marian Florescu,[1,*] Paul J. Steinhardt,[2,3] and Salvatore Torquato[2,3,4]
[1]*Advanced Technology Institute and Department of Physics, University of Surrey, Surrey, United Kingdom*
[2]*Department of Physics, Princeton University, Princeton, New Jersey 08544, USA*
[3]*Princeton Center for Theoretical Science, Princeton University, Princeton, New Jersey 08544, USA*
[4]*Department of Chemistry, Princeton University, Princeton, New Jersey 08544, USA*
(Received 17 February 2012; published 10 April 2013; corrected 12 April 2013)

Using finite-difference time domain and band structure computer simulations, we show that it is possible to construct optical cavities and waveguide architectures in hyperuniform disordered photonic solids that are unattainable in photonic crystals. The cavity modes can be classified according to the symmetry (monopole, dipole, quadrupole, etc.) of the confined electromagnetic wave pattern. Owing to the isotropy of the band-gap characteristics of hyperuniform disordered solids, high-quality waveguides with free-form geometries (e.g., arbitrary bending angles) can be constructed that are unprecedented in periodic or quasiperiodic solids. These capabilities have implications for many photonic applications.

DOI: 10.1103/PhysRevB.87.165116 PACS number(s): 41.20.Jb, 42.70.Qs, 78.66.Vs, 85.60.Jb

Recently, we introduced "hyperuniform stealthy" disordered photonic solids with large isotropic band gaps comparable in width to the anisotropic band gaps found in photonic crystals and capable of blocking light of all polarizations.[1] These solids challenge the conventional wisdom that band gaps require Bragg scattering and, hence, periodic or quasiperiodic order. The hyperuniform solids described in Ref. 1 demonstrate that Mie scattering is sufficient to generate band gaps provided the disorder is constrained to be hyperuniform (see definition below). We have explained how to design the dielectric materials in Ref. 1 and explored their band-gap and transport properties in Ref. 2.

In this paper, we explore the cavity and waveguide architectures possible in hyperuniform disordered (HD) solids. We find a wide range of confined cavity modes characterized by different approximate symmetries (monopole, dipole, quadrupole, etc.) and high-quality free-form waveguides that are possible because of the intrinsic isotropy of the solids and their band gaps.

Central to the class of materials considered in this paper is the concept of hyperuniformity, which was first introduced as an order metric for ranking point patterns according to their local density fluctuations at large length scales.[3] A point pattern in real space is hyperuniform if the number variance $\sigma^2(R)$ within a spherical sampling window of radius R (in d dimensions) grows more slowly than the window volume for large R, i.e., more slowly than R^d. Crystalline and quasicrystalline point patterns trivially satisfy this property, but it is also possible to have isotropic, disordered hyperuniform point patterns. In Fourier space, hyperuniformity means the structure factor $S(\mathbf{k})$ approaches zero as the wavenumber $|\mathbf{k}| \to 0$. The hyperuniform patterns that we consider are restricted to the subclass in which the number variance grows like the window surface area for large R, e.g., $\sigma^2(R) = AR$ in two-dimensions, or $\sigma^2(R) = AR^2$ in three dimensions, up to small oscillations.[3,4]

We further constrain the disorder to produce hyperuniform *stealthy* point patterns for which the structure factor $S(\mathbf{k})$ is isotropic and precisely equal to zero for a finite range of wave numbers $0 \leqslant k \leqslant k_C$ for some positive critical wave vector, k_C.[5] Hyperuniform photonic materials are then constructed by decorating a hyperuniform stealthy point pattern with dielectric materials according to the protocol described in Ref. 1. As a result of the constrained disorder, the HD photonic materials display an unusual combination of physical characteristics. Some are associated with typical disordered structures, such as statistical isotropy and multiple scattering resulting in localized states. Others, such as the existence of large and robust band gaps, result from a combination of hyperuniformity, uniform local topology (e.g., in two-dimensional, a network of vertices in which all connections are trivalent), and short-range geometric order (derived from the stealthiness).[1] Following our protocol, dielectric heterostructures with large, complete (both polarizations) band gaps have been designed. Recently, these designs have been fabricated on the microwave scale and successfully tested.[6]

The structures analyzed in this paper are generated by decorating hyperuniform point patterns with cylindrical rods with dielectric constant $\epsilon = 11.56$ and radius $r/a = 0.189$; these values are chosen to optimize the size of the photonic band gap. Here, the sample comprising N points is contained in a square box of size L, and we have introduced a length scale $a = L/\sqrt{N}$, such that the hyperuniform pattern has density of $1/a^2$. The hyperuniform point patterns are generated using the collective coordinate method in Ref. 3 with stealthy order parameter $\chi = 0.5$. It is notable that the photonic band gaps (PBGs) for these disordered structures are equivalent to the fundamental band gap in periodic systems; i.e., the spectral location of the gap is determined by the resonant frequencies of the scattering centers and always occurs between band N and $N + 1$, with N precisely the number of points per unit cell. A typical PBG size for structures with $\chi = 0.5$ is $\Delta\omega/\omega_C = 37\%$, where ω_C is the central frequency of the gap. Here, for simplicity, we consider PBGs for transverse magnetic (TM) polarized radiation.

We use the finite-difference time-domain (FDTD) method[7] to calculate the propagation of light inside the HD photonic structures.[2] We employ a computational domain with periodic boundary conditions in the transverse direction and perfectly matched layer (PML) condition in the normal direction. The

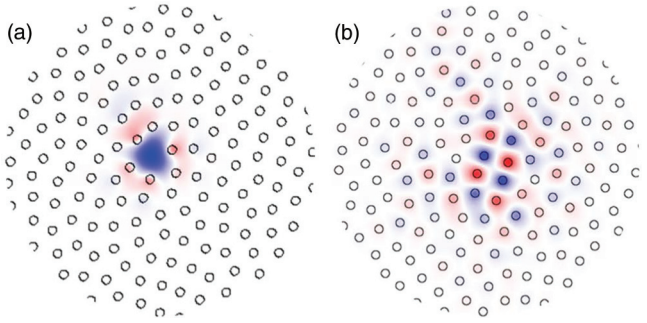

FIG. 1. (Color online) Electric field distribution for (a) a confined cavity mode in a hyperuniform disordered photonic structure introduced into the band gap by removing a dielectric cylinder from the original structure; to be compared with (b) a localized mode in the defect-free photonic structure. Note that the cavity mode has a shorter localization length.

spatial resolution in our numerical experiments is at least $n = 64$ mesh points per a, and the temporal resolution is $0.5/n \times a/c$, where c is the light speed in vacuum. For transmission calculations, a broadband source is placed at one end of the computational domain and the transmission signal is recorded at the other end with a line detector.[8] The Fourier components of the field are then evaluated and the spectra are averaged and normalized to the transmission profile in the absence of the structure. For quality factor calculations,[9] the modes are excited with a broadband pulse from a current placed directly inside the cavity and the simulation domain is surrounded by PML all around. After the source is turned off, the fields are analyzed, and frequencies and decay rates of the confined modes are evaluated.[8] To calculate photonic band structures, we employ a supercell approximation and use the conventional plane-wave expansion method.[10,11] In all the simulations performed in this work, the computational domain size is $\sqrt{N}a \times \sqrt{N}a$, with $N = 500$.

In an otherwise unperturbed HD structure, it is possible to create a localized state of the electromagnetic field by reducing or enhancing the dielectric constant at a certain point in the sample. In the two-dimensional structures considered here, this can be realized by removing one of the cylinders. Due to the presence of the point-like defect, a localized cavity mode is created within the photonic band gap at a certain frequency. Figure 1(a) shows a cavity mode obtained by removing one of the dielectric cylinders from a HD structure. We note that the electric field distribution is highly localized around the defect, extending only up to distances involving 1–2 rows of cylinders beyond the position of the missing cylinder. The quality factor of the two-dimensional confined mode is higher than 10^8. It is expected the for three-dimensional slab structures obtained by slab-configurations with a fine thickness, quality factors of at least 10^3 can be maintained, similar to the case of cavities in quasiperiodic photonic structures.[9] The nature of the localization mechanism around this type of defect in HD materials is rather different from the Anderson-like localization mechanism naturally present in this as well as conventional disordered structures. Figure 1 shows a localized photonic mode in the unperturbed HD structure has a localization length that is 5–6 times larger than that in the cavity mode.

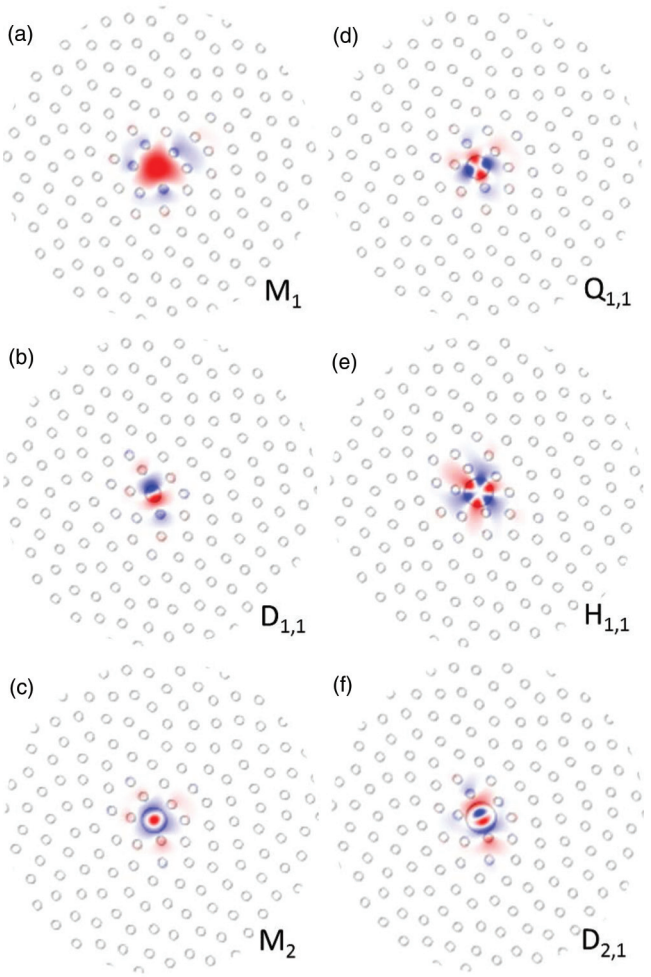

FIG. 2. (Color online) Electric field distribution for various cavity modes (defined in the text) obtained for different radii of the perturbed cylinder. From (a) to (f), the dimensionless defect radius r_d/r_0 takes the values 0,1.8,2.7,2.4,3.0,3.4, respectively.

We next study the evolution of the localized modes associated with a perturbed cylinder as its radius varies. When the radius of the cylinder is reduced, a single mode from the continuum of modes below the lower photonic band edge is pulled inside the PBG and becomes localized. If the radius of the cylinder is increased, a number of modes (the precise number is determined by the relative size of the defect cylinder) from the continuum of modes above the upper photonic band edge are pulled inside the PBG. Figure 2 shows the electric field mode distribution for a few selected localized modes. Note the nearly perfect monopole (M), dipolar (D), quadrupolar Q), and hexapolar (H) symmetries associated with certain modes. Different localized modes are indexed based on their approximate symmetry (M, D, H, . . .), where the first index refers to the order of the mode and the second index refers to the number of modes of a given order (e.g., $D_{1,2}$ is the second mode of first order with a dipole-like symmetry).

In Fig. 3 we show the evolution of the localized modes associated with a defect cylinder as a function of the dimensionless defect radius. Let us define the dimensionless defect radius to

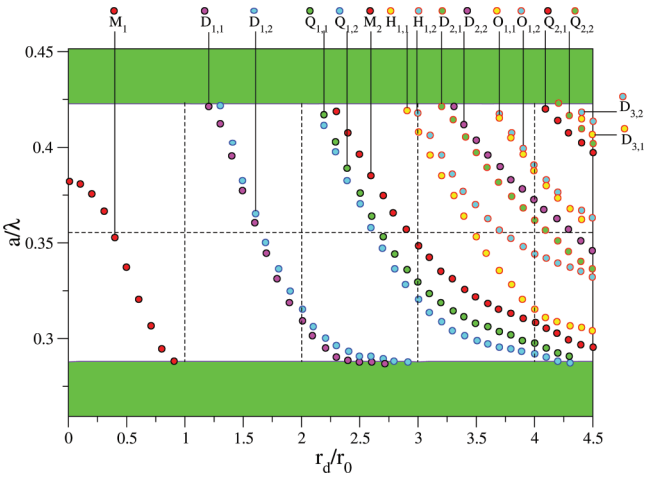

FIG. 3. (Color online) Photonic band structure calculations showing the evolution of localized modes associated with a defect cylinder as a function of the dimensionless defect radius r_d/r_0 (where $r_d/r_0 = 1$ corresponds to the unperturbed HD photonic structure). Different localized modes are labeled based on their approximate symmetry and order (e.g., $D_{1,2}$ indicates the second mode of first order with a dipole-like symmetry). The (green) shaded regions represent the continuum of modes that bound the PBG frequency range. For $r_d/r_0 < 1$ (the radius of the cylinder is decreased) only a single mode with a "monopole"is pushed up into the gap. For $r_d/r_0 > 1$ (the radius of the cylinder is increased), higher order modes are descending into the PBG. The electric field patterns for some of these modes are shown in Fig. 2.

be r_d/r_0. For a defect radius $r_d/r_0 = 0.47$ (where r_0 is the radius of the unperturbed cylinders), the defect mode reaches the midpoint of the PBG and is maximally protected from interactions with the propagating modes from the continua below and above the photonic band gap. When the radius of the defect cylinder is increased, it becomes possible to accommodate more localized modes in the defect region, distinguished either by their approximate symmetry or/and

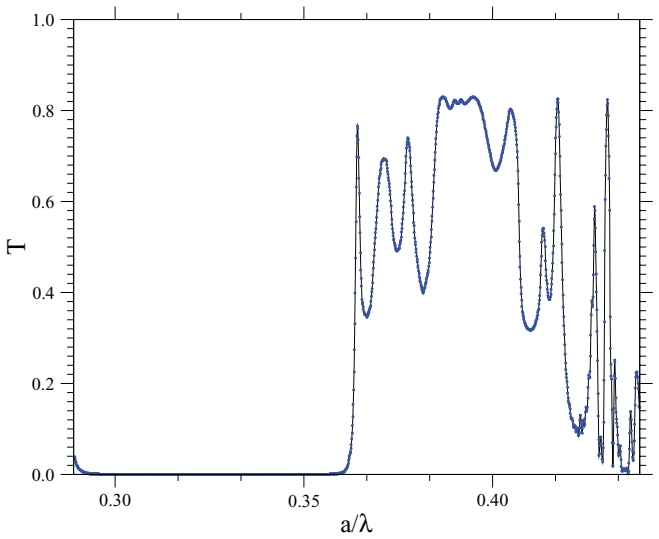

FIG. 4. (Color online) Transmission spectrum of a guided mode in a hyperuniform disordered photonic structure created by removing dielectric cylinders along a sinusoidally shaped path.

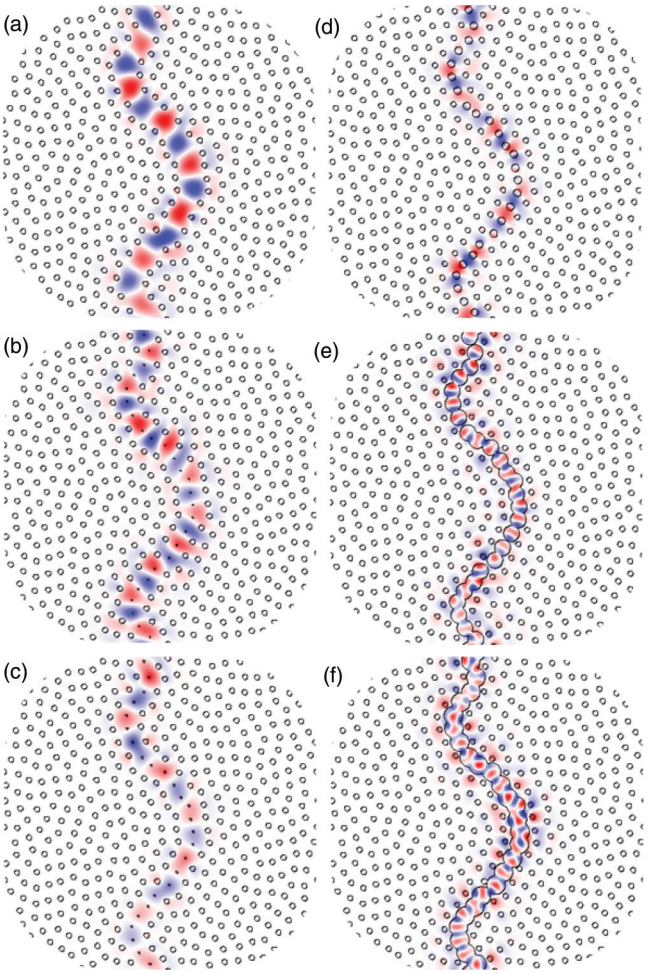

FIG. 5. (Color online) Electric field distribution for various guided modes obtained for different radii of the perturbed cylinders. From (a) to (f), the dimensionless defect radius r_d/r_0 takes the values 0,0.3,0.4,1.4,3.0,3.4, respectively.

frequency. For $r_d/r_0 = 4$, a total of 12 localized modes can coexist within the same defect. However, it should be noted that at at these large radii, the defect cylinders start to overlap with the surrounding cylinders and the confinement decreases.

We now consider waveguide architectures. In photonic crystals, removing a row of rods generates a channel through which light with frequencies within the band gap can propagate, a so-called crystal waveguide. Light cannot propagate elsewhere in the structure outside the channel because there are no allowed states. The waveguides must be composed of segments whose orientation is confined to the high-symmetry directions of the crystal. As a result, the waveguide bends of 60° or 90° can be easily achieved, but bends at an arbitrary angle lead to significant radiation loss due to excessively strong scattering at the bend junction and require additional engineering to function properly.

The existence of large and robust photonic band gaps in HD structures suggests that waveguiding should be possible in these noncrystalline photonic solids. An important difference is that the distribution of dielectric material around the bend junction is statistically isotropic. If the defect mode created by the removal of material falls within the PBG, the bend

can then be oriented at an arbitrary angle. In Fig. 5(a) we show an example of a guided mode obtained by removing dielectric cylinders along a sinusoidally shaped path through the HD structure. Remarkably, the light propagating through this unusually shaped waveguide channel is tightly confined in the transverse direction, penetrating only in the next few rows of dielectric cylinders. Our calculations show that the transmission reaches a maximum of about 83%; see Fig. 4. It is well known that in a photonic crystal, conservation of momentum due to the translation invariance along a linear waveguide prevents backscattering of the propagating mode. Such a mechanism is absent in any waveguide that presents deviations from linearity be it in a periodic or disordered structure, but it can be alleviated by optimizing the cylinder size along the waveguide channel.

The hyperuniform disordered structures analyzed here yield large photonic band gaps of around 40% of the central frequency, which in turn suggests that higher order guided modes can be excited in an appropriately designed waveguide channel. In Fig. 5, we also show higher order guided modes that are obtained by varying the radius of the defect cylinders along the channel path.

In summary, we have introduced architectures for the design of optical cavities and waveguides in hyperuniform disordered materials. We have demonstrated that point-like defects can support localized modes with a variety of symmetries and multiple frequencies. By exploiting the isotropy of the PBG unique to hyperuniform disordered structures, we have also shown that it is possible to design waveguides of essentially arbitrary shape, along which the light can be guided through the excitation of localized resonances similar to the ones that we found in the point-like defects. The ability to localize modes of different symmetry and frequency in the same physical cavity and to guide light through modes with different localization properties can have a great impact on all-optical switching, single-atom laser and solar cell systems.[12–14] The new cavity and waveguide architectures are promising candidates for achieving highly flexible and robust platforms for integrated optical microcircuitry.

While the present study deals only with TM polarized radiation, qualitatively similar results can be obtained for transverse electric (TE) polarized radiation for structures designed using the constrained optimization protocol developed in Ref. 1. This will be the subject of a future investigation.

This work was supported by the National Science Foundation under Grants No. DMR-0606415 and No. ECCS-1041083. M.F. also acknowledges support from the University of Surrey FRSF and Santander awards.

*Electronic address: m.florescu@surrey.ac.uk

[1] M. Florescu, S. Torquato, and P. J. Steinhardt, Proc. Natl. Acad. Sci. USA **106**, 20658 (2009).
[2] M. Florescu, P. J. Steinhardt, and S. Torquato (unpublished).
[3] S. Torquato and F. H. Stillinger, Phys. Rev. E **68**, 041113 (2003).
[4] C. E. Zachary and S. Torquato, J. Stat. Mech.: Theory Exp. (2009) P12015.
[5] R. D. Batten, F. H. Stillinger, and S. Torquato, J. Appl. Phys. **104**, 033504 (2008).
[6] W. Man, M. Florescu, K. Matsuyama, P. Yadak, S. Torquato, P. J. Steinhardt, and P. Chaikin, CLEO, OSA Technical Digest (CD), Optical Society of America, 2010, paper CThS2.
[7] K. Yee, IEEE Trans. Antennas Propag. **14**, 302 (1966).
[8] A. F. Oskooi, D. Roundy, M. Ibanescu, P. Bermel, J. D. Joannopoulos, and S. G. Johnson, Comput. Phys. Commun. **181**, 687 (2010).
[9] W. T. M. Irvine, K. Hennessy, and D. Bouwmeester, Phys. Rev. Lett. **96**, 057405 (2006).
[10] S. G. Johnson and J. D. Joannopoulos, Opt. Express **8**, 173 (2001).
[11] L. Wu, F. Zhuang, and S. He, Phys. Rev. E **67**, 026612 (2003).
[12] M. Florescu and S. John, Phys. Rev. A **69**, 053810 (2004).
[13] L. Florescu, S. John, T. Quang, and R. Z. Wang, Phys. Rev. A **69**, 013816 (2004).
[14] M. Florescu, K. Busch, and J. P. Dowling, Phys. Rev. B **75**, 201101(R) (2007).